

Exchange Control of Nuclear Spin Diffusion in a Double Quantum Dot

D. J. Reilly¹, J. M. Taylor², J. R. Petta³, C. M. Marcus¹, M. P. Hanson⁴ and A. C. Gossard⁴

¹ Department of Physics, Harvard University, Cambridge, MA 02138, USA

² Department of Physics, Massachusetts Institute of Technology, Cambridge, MA 02139, USA

³ Department of Physics, Princeton University, Princeton, NJ 08544, USA and

⁴ Department of Materials, University of California, Santa Barbara, California 93106, USA

Coherent two-level systems, or qubits, based on electron spins in GaAs quantum dots are strongly coupled to the nuclear spins of the host lattice via the hyperfine interaction [1, 2, 3, 4, 5]. Realizing nuclear spin control would likely improve electron spin coherence and potentially enable the nuclear environment to be harnessed for the long-term storage of quantum information [6, 7]. Toward this goal, we report experimental control of the relaxation of nuclear spin polarization in a gate-defined two-electron GaAs double quantum dot. A cyclic gate-pulse sequence transfers the spin of an electron pair to the host nuclear system, establishing a local nuclear polarization that relaxes on a time scale of seconds. We find nuclear relaxation depends on magnetic field and gate-controlled two-electron exchange, consistent with a model of electron-mediated nuclear spin diffusion.

Dynamic nuclear polarization (DNP), in which the ‘flip’ of a polarized electron spin is accompanied by the simultaneous ‘flop’ of a nuclear spin [9], has served as a probe of nuclear dynamics in bulk semiconductors [10, 11], confined semiconductor devices, and optical systems [12, 13, 14, 15, 16, 17, 18]. In quantum dots, hyperfine coupling with electron spins can lead to nuclear dynamics distinct from those of bulk materials. For instance, using optical techniques, the presence of a single residual electron in an InGaAs dot was recently shown to significantly enhance the decay of nuclear polarization [15]. Signatures of DNP have also been investigated in transport through few-electron double quantum dots. In this case, spin blockade can lead to a complex interplay between electron and nuclear spin transitions, resulting in bi-stability, hysteresis, and long-time oscillations of leakage currents [19, 20, 21, 22, 23]. Understanding the coupled evolution of the electron-nuclear system is important for the development of long-lived qubits based on these devices.

In this Letter, we report time-resolved measurements investigating the induction and relaxation of DNP in a few-electron double quantum dot as a function of magnetic field and charge arrangement. Cyclic evolution of the two-electron spin state, driven by gate pulses [24], repeatedly flops nuclear spins to create a small local DNP of order 1%. Relaxation is monitored by detecting the Overhauser field using high-bandwidth proximal charge sensing [25]. From the long nuclear relaxation times we conclude that the modest polarization achieved

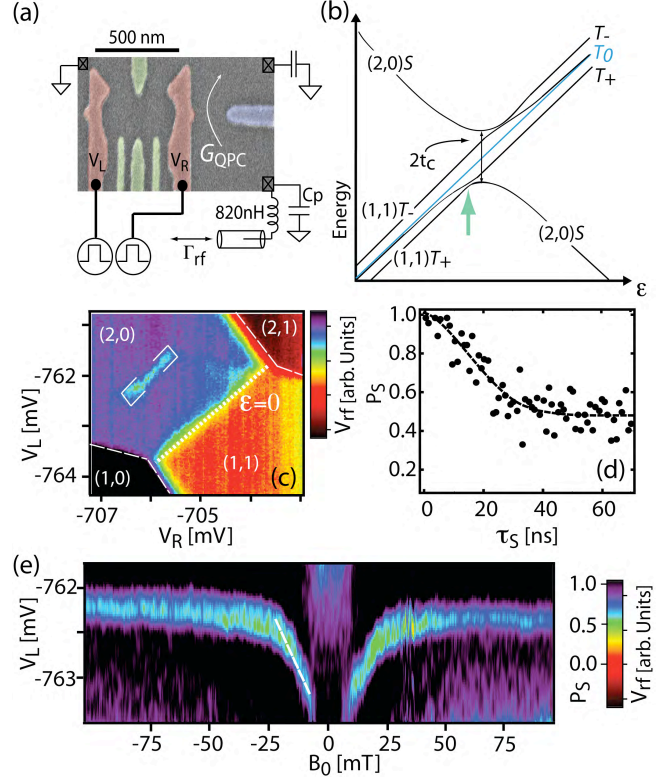


FIG. 1: (a) False-color SEM image of a representative double-dot with integrated rf-QPC charge sensor. Changes in QPC conductance are mapped to changes in reflected rf power from an impedance matching network based on series inductor (820 nH) and paracitic capacitance $C_p \sim 0.6$ pF. (b) Energy level diagram of the two-electron system. Labels (n,m) define the number of electrons in the left and right dot. Green arrow points to the $S-T_+$ avoided crossing. (c) V_{rf} around the (2,0)-(1,1) charge transition during cycling of the probe sequence. A plane has been subtracted. The region indicated with white lines corresponds to the $S-T_+$ resonance. $B_0 = 8$ mT. (d) Singlet return probability P_S as a function of separation time τ_S yielding a $T_2^* \sim 15$ ns. $B_0 = 8$ mT, $\tau_M = 1.6$ μ s. Black dashed line is a fit to the theoretical gaussian form [8]. (e) P_S as a function of left gate bias V_L and magnetic field B_0 . Dashed white line is used to convert position of the resonance in V_L to B_{tot} .

is not limited by nuclear spin out-diffusion, but rather likely arise from a saturation in the flip-flop efficiency of the pumping cycle. The present work advances previous studies by demonstrating that nuclear diffusion can be made sensitive to the exchange coupling of confined

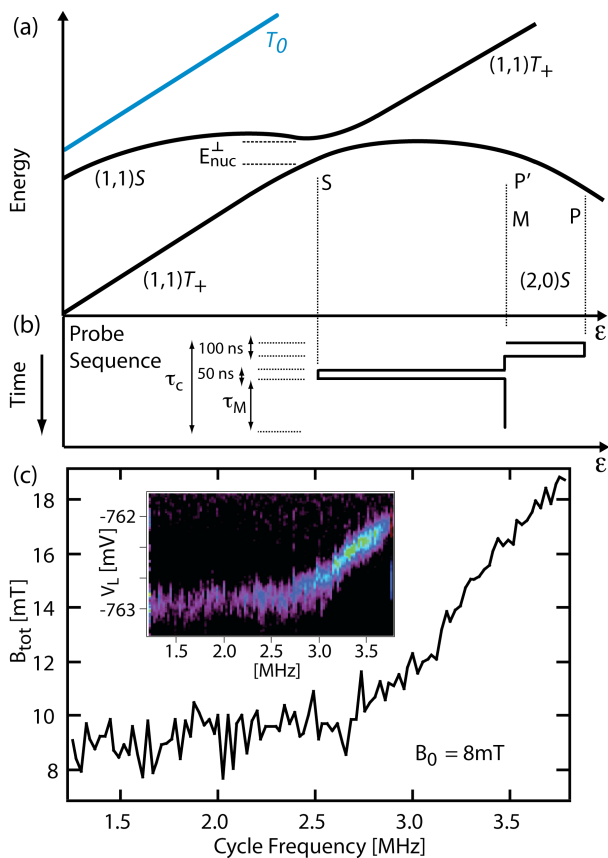


FIG. 2: (a) Energy level diagram near the $S - T_+$ resonance. (b) Pulse cycle used to measure the position of the resonance during the “probe” sequence. (c) Inset: Position of $S - T_+$ resonance with respect to gate bias, V_L . Color scale is the same as Fig. 1(e). For cycle rates below 1 MHz, the position of the resonance indicates $B_{\text{tot}} \sim B_0$, i.e., no appreciable polarization is established by the process of measuring the position of the $S - T_+$ resonance. The main panel shows the position of the resonance converted to units of magnetic field via the calibration in Fig. 1(e).

electrons, controlled experimentally through the spatial charge arrangement with fixed total charge. Finally, we infer from magnetic field and charge-arrangement dependences that electron-mediated coupling of nuclear spins [9, 29, 31] is the dominant contribution to the nuclear polarization diffusion rate.

The double quantum dot is formed by Ti/Au gates patterned with electron beam lithography on the surface of a GaAs/Al_{0.3}Ga_{0.7}As heterostructure with two dimensional electron gas (2DEG) with density $2 \times 10^{15} \text{ m}^{-2}$ and mobility $20 \text{ m}^2/\text{Vs}$, as shown in Fig. 1(a). Measurements were made in a dilution refrigerator at the base electron temperature of $\sim 120 \text{ mK}$. A schematic energy level diagram of the two-electron system is shown in Fig. 1(b), with the labels (n,m) giving the number of electrons in the left and right dot. Quasistatic gate voltages control interdot tunnel coupling, t_c , while the detuning, ϵ , from the (2,0)-(1,1) charge degeneracy is controlled on nanosecond time scales using fast pulses applied to the

gates marked in red in Fig. 1(a). The charge configuration of the double dot is detected by monitoring the conductance G_{QPC} of a proximal rf quantum point contact (rf-QPC). G_{QPC} controls the reflected power Γ_{rf} of a 220 MHz rf-carrier; following demodulation, this yields a voltage V_{rf} that constitutes the charge sensing signal [25].

The effective total field experienced by electrons in (1,1) is given by $\mathbf{B}_{\text{tot}} = \mathbf{B}_0 + \mathbf{B}_{\text{nuc}}$, where \mathbf{B}_0 is the external field applied perpendicular to the 2DEG plane and $\mathbf{B}_{\text{nuc}} = (\mathbf{B}_{\text{nuc}}^L + \mathbf{B}_{\text{nuc}}^R)/2$ is the Overhauser field averaged over left and right dots. The avoided crossing between the singlet (S) and the (1,1) $m_s = 1$ triplet (T_+) occurs at a value of ϵ (green arrow in Fig. 1(b)) set by the total Zeeman energy, $E_{\text{tot}} = g\mu_B B_{\text{tot}}$, where $g \simeq -0.4$ is the electron g-factor in GaAs, μ_B is the Bohr magneton, and B_{tot} is the magnitude of \mathbf{B}_{tot} . The gap and width of the avoided crossing are set by $E_{\text{nuc}}^\perp = g\mu_B \Delta B_{\text{nuc}}^\perp$, where $\Delta B_{\text{nuc}}^\perp$ is the magnitude of the component of $\Delta \mathbf{B}_{\text{nuc}} = (\mathbf{B}_{\text{nuc}}^L - \mathbf{B}_{\text{nuc}}^R)/2$ transverse to \mathbf{B}_{tot} .

We probe the $S - T_+$ resonance using the pulse sequence shown in Fig. 2(b), which first prepares (2,0) S at (P) then separates the electrons (S) for a time τ_S before returning to (2,0) for measurement (M) for time $\tau_M \sim 5 \mu\text{s}$. Pauli spin-blockade ensures that only the (1,1) singlet returns to (2,0), with triplets blocked for a time T_1 . In this way, the two-electron spin-state is mapped to a charge configuration that is detected with the rf-QPC. Cycling this sequence yields a feature at (M) in the (2,0) region, indicated by white lines in Fig. 1(c). Once calibrated, V_{rf} gives the probability $1 - P_S$ that an initial singlet evolved into T_+ during the separation interval τ_S . V_{rf} is calibrated using the measured values in (2,0) and (1,1) to define $P_S = 1$ and $P_S = 0$, giving the scale bar in Fig. 1(e). Fitting the time-averaged function $P_S(\tau_S)$ gives an inhomogeneous dephasing time, $T_2^* \sim 15 \text{ ns}$. The dependence of the $S - T_+$ resonance position (in V_L , with V_R fixed) on B_0 in the range $B_0 = 5 - 18 \text{ mT}$, in the absence of a time-averaged nuclear polarization, serves as a calibration used to determine B_{tot} when nuclear polarization is present [26].

Dynamic nuclear polarization is investigated using a three-step “pump-pause-probe” sequence: The pump sequence starts from a singlet in (2,0) then moves adiabatically through the $S - T_+$ resonance, flipping an electron and flopping a nuclear spin, in principle once per cycle at a rate of 4 MHz [24]. The “probe” sequence (Fig. 2(a,b)) also starts with a singlet in (2,0) but moves to the $S - T_+$ resonance, providing a measure of B_{tot} . For a cycle rate below 1 MHz, the probe sequence does not induce nuclear polarization, as seen in Fig. 2(c). For all DNP data shown, the cycle rate of the probe sequence was 200 kHz. Pump and probe cycles are separated by a static “pause” of duration Δt .

The pump sequence creates a steady-state DNP of order $\sim 10 \text{ mT}$, which, in the absence of a pause, relaxes during the probing cycle on a time scale $\tau_R = 8 \text{ s}$, found

by fitting an exponential to $B_{\text{tot}}(t)$ (Fig. 3(c)). Increasing B_0 from 8 mT to 10 mT doubles the time taken for B_{tot} to return to B_0 . At $B_0 = 15$ mT, B_{tot} relaxes over a time scale similar to the $B_0 = 10$ mT data. We note that at $t = 0$, B_{tot} appears nearly independent of B_0 . This suggests that the pump sequence ceases to produce polarization above a certain value of B_{tot} , consistent with previous measurements [24]. The measured relaxation rate cannot account for the small steady-state polarization (~ 10 mT), and we are led to conclude that there must be significant decrease in the efficiency of the polarization cycle with increasing B_{nuc} .

The effect of pausing in (2,0) between the pump and probe sequences can be seen in Fig. 4(b), which shows that more than half the polarization remains after pausing for 30 s in (2,0)S (Fig. 4(c)). Once the probe sequence is initiated after the pause, B_{tot} once again decays with $\tau_R \sim 8$ s. The influence of the probe sequence is examined further by introducing multiple pause intervals in (2,0), interleaved with probe cycles (Fig. 4(d)).

The dependence of the nuclear relaxation rate on the two-electron spin-state during the pause duration is shown in Fig. 4(f). Pausing for the duration of Δt in the (2,0) state yields a relaxation time $\tau_R = 56$ s (red data in Fig. 4(f)), while pausing in (1,1) yields $\tau_R = 26$ s (green data in Fig. 4(f)) [27]. We ascribe these different relaxation times to a nuclear spin diffusion constant that depends on the two-electron spin state. With diffusion dominated by the shortest dimension of the dot, perpendicular to the electron gas, we approximate the diffusion constant $D = d^2/\tau_R$ based on an estimate of the width of the wavefunction $d \sim 7.5$ nm [28]. This gives $D \sim 1 \times 10^{-14}$ cm²s⁻¹ for the case of pausing in (2,0), consistent with estimates of diffusion by nuclear dipole-dipole flipping [11]. Activation of the probe sequence increases diffusion to $D \sim 7 \times 10^{-14}$ cm²s⁻¹.

The two-electron spin state is expected to affect nuclear spin diffusion in two opposing ways. The presence of strongly confined electrons creates an inhomogeneous Knight shift [3], lifting the degeneracy between nuclear dipoles and suppressing diffusion by dipolar flipping. Competing with this mechanism is the enhancement of diffusion via electron-mediated nuclear spin exchange [9]. We first estimate the magnitude of each of these mechanisms in an effort to explain the different diffusion rates observed in (1,1) and (2,0). For our device we estimate that the Knight shift alone suppresses diffusion by at most 10 % (see Supplementary Information). Indirect nuclear-spin exchange occurs when a nuclear spin, contributing to $\Delta \mathbf{B}_{\text{nuc}}^\perp$, flips the electron spin, which, upon flipping back generally flops a different nuclear spin [29, 31]. This virtual process of nuclear-spin exchange is suppressed by the electron Zeeman energy and is thus dependent on B_{tot} . We note that mediated flipping operates on nuclear spins within the dot, enhancing diffusion from the center to the edge, where dipolar diffusion beyond the dot begins to dominate. We find (see Supplementary Information) that for $B_{\text{tot}} \lesssim 10$ mT, $B_{\text{nuc}} \sim 20$ mT,

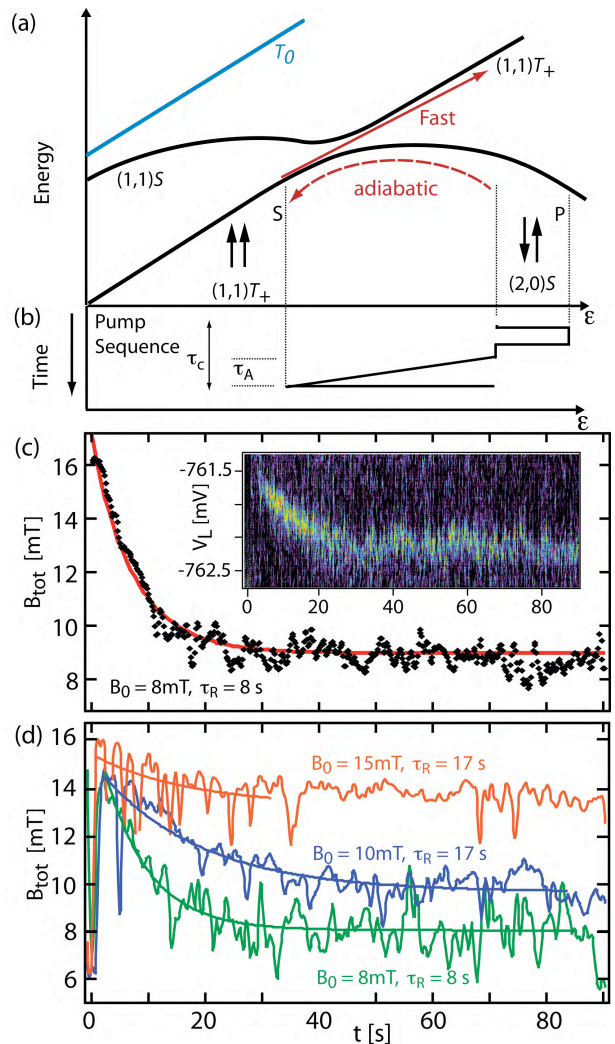


FIG. 3: (a) Energy level diagram near the $S - T_+$ avoided-crossing with pump sequence used to create a DNP shown in (b), $\tau_A = 50$ ns, $\tau_c = 250$ ns. Pump cycle rate is 4 MHz. (c) Inset: Decay in the position of the resonance with respect to V_L following pumping. Main panel shows the average of five pump-probe sequences, with B_{tot} calibrated using Fig. 1(e). Red curve is an exponential fit. (d) Relaxation of DNP at $B_0 = 8$ mT (green) $\tau_R = 8 \pm 2$ s, $B_0 = 10$ mT (blue) $\tau_R = 17 \pm 3$ s, and $B_0 = 15$ mT (red) $\tau_R = 17 \pm 5$ s. For the $B_0 = 15$ mT data we constrain the fit to the first 30 s due to the small available polarization signal. Noise in the resonance position exaggerates τ_R to 22 s when fitting over the total data range.

the enhancement of diffusion via electron-mediated spin flips in the (1,1) state dominates the suppression of diffusion due to the Knight shift, leading to an overall increase in nuclear spin diffusion. However, with electrons in (2,0)S, both hyperfine mechanisms are suppressed by the electron exchange energy J , which is 10^4 times larger than $g\mu_B B_{\text{tot}}$ for the fields used in these experiments. In particular, electron-mediated (enhanced) diffusion is a negligible contribution and the dynamics of B_{tot} are governed solely by the bare dipole-dipole diffusion of polarization from the dot [30].

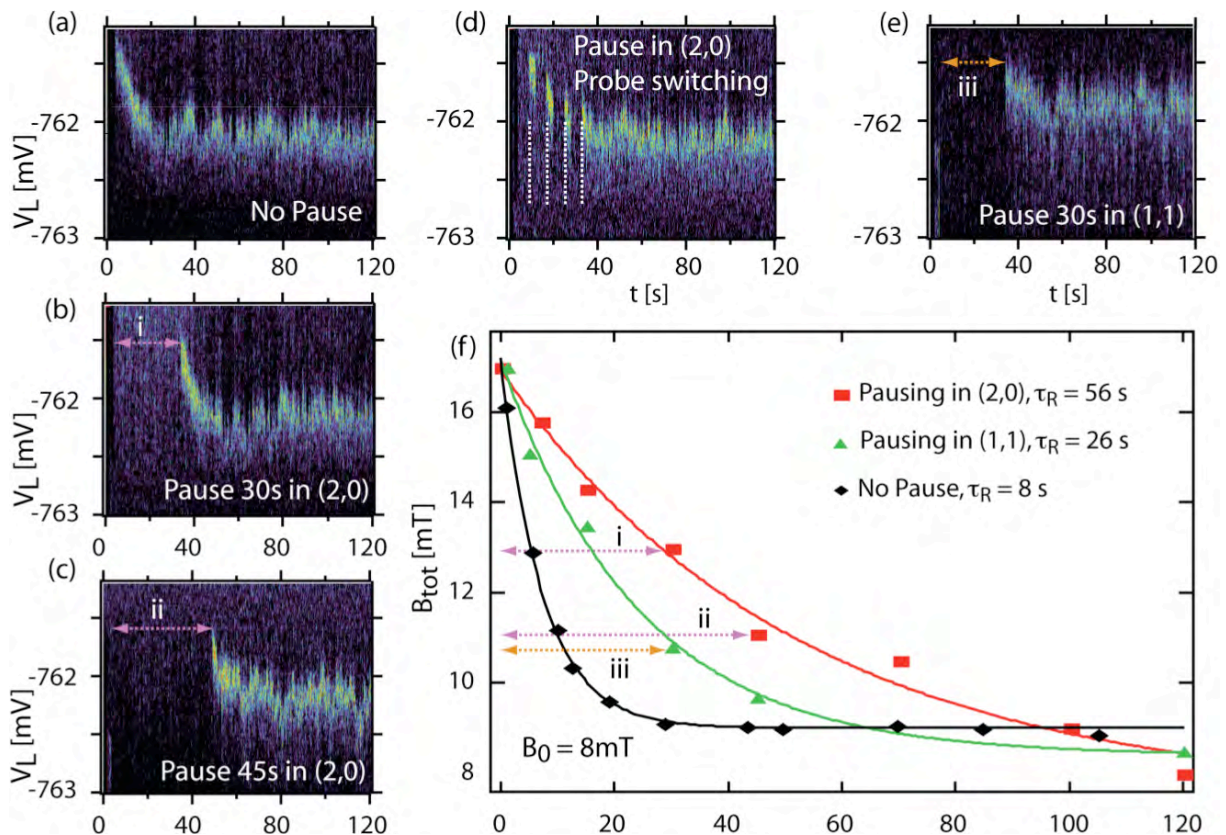


FIG. 4: (a) Immediate decay in the position of the resonance during the probe sequence. (b) Decay in position of the resonance following a pause interval of 30 s in (2,0) between the pump and probe sequences. Pausing in (2,0) suppresses hyperfine coupling. (c) Same as (b), but with pause interval set to 45 s. (d) Decay of resonance during probing, interleaved with multiple pause intervals. (e) Decay in position of resonance following a pause of 30 s in (1,1). (f) Decay of B_{tot} as a function of pause interval Δt and for different configurations of two-electron spin state.

Electron mediated flipping leads to an increase in diffusion with decreasing B_{tot} , consistent with the B_0 dependence of the data shown in Fig. 3(d). Non-secular corrections to the nuclear dipole-dipole interaction will also enhance diffusion for $B_{\text{tot}} \lesssim 1$ mT [9, 15], but these are suppressed at the applied fields used in our experiment. Flipping of spins via co-tunneling is estimated to be a negligible based on a measurement of electron spin relaxation ($T_1 \sim 15\mu\text{s}$) in this device. At the $S - T_+$ resonance, exchange and the electron Zeeman energy effectively “cancel” allowing rapid flipping of electrons that readily mediate rapid exchange of nuclear spins. This is the likely explanation for the enhanced diffusion observed during the probe sequence.

Hyperfine mediated nuclear dynamics in quantum dots have been considered theoretically in the context of spin-preserving processes [2, 3, 4, 5, 29, 31], but measurement of the time scales for nuclear relaxation in dots containing a single electron have only recently been reported [15]. For two-electron systems, the measurements presented here bring to light the role of electron exchange,

which as we have shown can lead to a suppression of hyperfine-mediated nuclear spin diffusion. Finally, based on our measurement of τ_R , we emphasize that the maximum steady-state DNP ~ 10 mT cannot be limited by rapid out diffusion. Rather, these results indicate that the pump sequence strongly decreases in efficiency with increasing polarization, consistent with previous measurements [24] and the idea of dark state formation [32]. We anticipate that these results will be of relevance in the construction of protocols to suppress spin dephasing and in the development of schemes for imprinting electron spin states on nuclear memory.

We thank Leo DiCarlo, Alex Johnson, and Edward Laird for technical contributions. We thank Bill Coish, Frank Koppens, Daniel Loss, and Amir Yacoby for useful discussion. This work was supported by ARO/IARPA, DARPA, NSF-NIRT (EIA-0210736), the Harvard Center for Nanoscale Systems, and a Pappalardo fellowship (JMT). Research at UCSB supported in part by QuEST, an NSF Center.

-
- [1] J. R. Petta et al., Coherent manipulation of coupled electron spins in semiconductor quantum dots. *Science* **309**, 2180 (2005).
- [2] S. I. Erlingsson, Y. V. Nazarov, and V. I. Fal'ko, Nucleus-mediated spin-flip transitions in GaAs quantum dots. *Phys. Rev. B* **64**, 195306 (2001).
- [3] A. V. Khaetskii, D. Loss, and L. Glazman, Electron spin decoherence in quantum dots due to interaction with nuclei. *Phys. Rev. Lett.* **88**, 186802 (2002).
- [4] I. A. Merkulov, A. L. Efros, and M. Rosen, Electron spin relaxation by nuclei in semiconductor quantum dots. *Phys. Rev. B* **65**, 205309 (2002).
- [5] W. M. Witzel and S. Das Sarma, Quantum theory for electron spin decoherence induced by nuclear spin dynamics in semiconductor quantum computer architectures: Spectral diffusion of localized electron spins in the nuclear solid-state environment. *Phys. Rev. B* **74**, 035322 (2006).
- [6] J. M. Taylor, C. M. Marcus, and M. D. Lukin, Long-lived memory for mesoscopic quantum bits. *Phys. Rev. Lett.* **90**, 206803 (2003).
- [7] W. M. Witzel and S. D. Sarma, Nuclear spins as quantum memory in semiconductor nanostructures. *Phys. Rev. B* **76**, 045218 (2007).
- [8] J. M. Taylor et al., Relaxation, dephasing, and quantum control of electron spins in double quantum dots. *Phys. Rev. B* **76**, 035315 (2007).
- [9] A. Abragam, *Principles of Nuclear Magnetism (International Series of Monographs on Physics) Oxford University Press, USA* (1983).
- [10] G. Lampel, Nuclear dynamic polarization by optical electronic saturation and optical pumping in semiconductors. *Phys. Rev. Lett.* **20**, 491 (1968).
- [11] D. Paget, Optical detection of NMR in high-purity GaAs: Direct study of the relaxation of nuclei close to shallow donors. *Phys. Rev. B* **25**, 4444 (1982).
- [12] G. Salis et al., Optical manipulation of nuclear spin by a two-dimensional electron gas. *Phys. Rev. Lett.* **86**, 2677 (2001).
- [13] K. Wald et al., Local dynamic nuclear polarization using quantum point contacts. *Phys. Rev. Lett.* **73**, 1011 (1994).
- [14] M. Dobers et al., Electrical detection of nuclear magnetic resonance in GaAs-AlxGa1-xAs heterostructures. *Phys. Rev. Lett.* **61**, 1650 (1988).
- [15] P. Maletinsky, A. Badolato, and A. Imamoglu, Dynamics of quantum dot nuclear spin polarization controlled by a single electron. *Phys. Rev. Lett.* **99**, 056804 (2007).
- [16] D. Gammon et al., Electron and nuclear spin interactions in the optical spectra of single GaAs quantum dots. *Phys. Rev. Lett.* **86**, 5176 (2001).
- [17] C. W. Lai et al., Knight-field-enabled nuclear spin polarization in single quantum dots. *Phys. Rev. Lett.* **96**, 167403 (2006).
- [18] A. I. Tartakovskii et al., Nuclear spin switch in semiconductor quantum dots. *Phys. Rev. Lett.* **98**, 26806 (2007).
- [19] K. Ono and S. Tarucha, Nuclear-spin-induced oscillatory current in spin-blockaded quantum dots. *Phys. Rev. Lett.* **92**, 256803 (2004).
- [20] F. H. L. Koppens et al., Control and detection of singlet-triplet mixing in a random nuclear field. *Science* **309**, 1346 (2005).
- [21] J. Baugh et al., Large Nuclear Overhauser Fields Detected in Vertically Coupled Double Quantum Dots. *Phys. Rev. Lett.* **99**, 096804 (2007).
- [22] O. N. Jouravlev and Y. V. Nazarov, Electron Transport in a Double Quantum Dot Governed by a Nuclear Magnetic Field. *Phys. Rev. Lett.* **99**, 176804 (2006).
- [23] M. S. Rudner and L. S. Levitov, Electrically driven reverse Overhauser pumping of nuclear spins in quantum dots. *Phys. Rev. Lett.* **99**, 246602 (2007).
- [24] J. R. Petta et al., Dynamic nuclear polarization with single electron spins. *Phys. Rev. Lett.* **100**, 067601 (2008).
- [25] D. J. Reilly et al., Fast single-charge sensing with an rf quantum point contact. *App. Phys. Lett.* **91**, 162101 (2007).
- [26] Although the true functional form relating the position of the resonance to B_0 is a power-law, a linear dependence fits the data well over the range of polarization accessed in this experiment.
- [27] A re-calibration is required to account for a slight shift in the position of the resonance during pausing in (1,1).
- [28] M. Stopa, Private communication, (2007).
- [29] W. A. Coish and D. Loss, Singlet-triplet decoherence due to nuclear spins in a double quantum dot. *Phys. Rev. B* **72**, 125337 (2005).
- [30] John. A. McNeil and W. Gilbert Clark, Nuclear quadrupolar spin-lattice relaxation in some III-V compounds. *Phys. Rev. B* **13**, 4705 (1976).
- [31] W. Yao, R.-B. Liu, and L. J. Sham, Theory of electron spin decoherence by interacting nuclear spins in a quantum dot. *Phys. Rev. B* **74**, 195301 (2006).
- [32] A. Imamoglu, et al., Optical pumping of quantum-dot nuclear spins. *Phys. Rev. Lett.* **91**, 017402 (2003).